

**Experimental determination of the Lorenz number in  $\text{Cu}_{0.01}\text{Bi}_2\text{Te}_{2.7}\text{Se}_{0.3}$  and  $\text{Bi}_{0.88}\text{Sb}_{0.12}$** K. C. Lukas,<sup>1</sup> W. S. Liu,<sup>1</sup> G. Joshi,<sup>1</sup> M. Zebarjadi,<sup>2</sup> M. S. Dresselhaus,<sup>3</sup> Z. F. Ren,<sup>1</sup> G. Chen,<sup>2</sup> and C. P. Opeil<sup>1</sup><sup>1</sup>*Department of Physics, Boston College, Chestnut Hill, Massachusetts 02467, USA*<sup>2</sup>*Department of Mechanical Engineering and Computer Science, Massachusetts Institute of Technology, Cambridge, Massachusetts 02139, USA*<sup>3</sup>*Department of Physics and Department of Electrical Engineering and Computer Science, Massachusetts Institute of Technology, Cambridge, Massachusetts 02139, USA*

(Received 3 January 2012; revised manuscript received 6 April 2012; published 7 May 2012)

Nanostructuring has been shown to be an effective approach to reduce the lattice thermal conductivity and improve the thermoelectric figure of merit. Because the experimentally measured thermal conductivity includes contributions from both carriers and phonons, separating out the phonon contribution has been difficult and is mostly based on estimating the electronic contributions using the Wiedemann-Franz law. In this paper, an experimental method to directly measure electronic contributions to the thermal conductivity is presented and applied to  $\text{Cu}_{0.01}\text{Bi}_2\text{Te}_{2.7}\text{Se}_{0.3}$ ,  $[\text{Cu}_{0.01}\text{Bi}_2\text{Te}_{2.7}\text{Se}_{0.3}]_{0.98}\text{Ni}_{0.02}$ , and  $\text{Bi}_{0.88}\text{Sb}_{0.12}$ . By measuring the thermal conductivity under magnetic field, electronic contributions to thermal conductivity can be extracted, leading to knowledge of the Lorenz number in thermoelectric materials.

DOI: [10.1103/PhysRevB.85.205410](https://doi.org/10.1103/PhysRevB.85.205410)

PACS number(s): 72.15.Jf, 72.20.Pa, 66.70.Df

**I. INTRODUCTION**

The determination of the Lorenz number is an important aspect in thermoelectric research due to the fact that  $ZT$  enhancement is being realized through the reduction of thermal conductivity, specifically focusing on reducing the lattice portion of the thermal conductivity. The total thermal conductivity is given by

$$\kappa_{\text{total}} = \kappa_{\text{carrier}} + \kappa_{\text{lattice}}, \quad (1)$$

where  $\kappa_{\text{carrier}}$  and  $\kappa_{\text{lattice}}$  are the contributions to the thermal conductivity from the carriers and the lattice, respectively. Since only the total thermal conductivity can be measured, the contributions must be separated in some way. This is done using the Wiedemann-Franz law and by defining a Lorenz number  $L$ , which is the given by

$$L = \frac{\kappa_{\text{carrier}}}{\sigma T}, \quad (2)$$

where  $\sigma$  is the electrical conductivity and  $T$  is the absolute temperature. In metals the Lorenz number can be determined by measuring the electrical conductivity and total thermal conductivity at a given temperature, from which the Lorenz number is calculated using Eq. (2). This method is only useful in metals where the total thermal conductivity is approximately equal to  $\kappa_{\text{carrier}}$ . For the classical free-electron model the Lorenz number is given as  $2.44 \times 10^{-8} \text{ V}^2 \text{ K}^{-2}$ .<sup>1</sup> It is important to note that the Lorenz number, as described by the free-electron model, is not an accurate value for most materials and in a given material depends on the detailed band structure, position of the Fermi level, and the temperature; for semiconductors this relates to the carrier concentration. Therefore, when  $\kappa_{\text{lattice}}$  and  $\kappa_{\text{carrier}}$  become comparable to each other, there must be a method for differentiating between the two components of  $\kappa_{\text{total}}$ . To date the separation of the two components has been accomplished through calculation by approximating the Lorenz number, and hence the carrier contribution, through various different formalisms.<sup>1,3,4</sup> Determinations of the Lorenz

number have also been made experimentally;<sup>1</sup> however, there are few.

In order to separate  $\kappa_{\text{lattice}}$  and  $\kappa_{\text{carrier}}$  experimentally, two approaches have been used to determine the Lorenz number. Both methods utilize a transverse magnetic field in order to suppress the electronic component of the thermal conductivity. One approach uses a classically large magnetic field, while the other is performed in intermediate fields. A classically large magnetic field is described as  $\mu B \gg 1$ , where  $\mu$  is the carrier mobility and  $B$  is the magnetic field.<sup>1</sup> When this limit is reached, the electronic component of  $\kappa$  is completely suppressed so that the measurement yields only the lattice portion of the thermal conductivity, from which  $\kappa_{\text{carrier}}$  and hence the Lorenz number can be calculated using Eqs. (1) and (2).

Very often it is difficult to reach a classically large field, making this type of measurement impossible, and therefore other methods have been developed for determining  $L$ . For example, Goldsmid *et al.* developed a magnetothermal resistance (MTR) method for extracting the Lorenz number at lower magnetic fields, specifically in the region where  $\mu B \approx 1$ .<sup>5-8</sup> In the MTR method the sample is kept at a constant temperature while the field is varied. In this case both the electrical conductivity and the total thermal conductivity will change with the field due to the Lorentz force acting on the carriers, which is induced by the transverse magnetic field. Equation (1) can be rewritten in the form

$$\kappa(B)_{\text{total}} = LT\sigma(B) + \kappa_{\text{lattice}}, \quad (3)$$

where now both  $\kappa$  and  $\sigma$  are dependent on the magnetic field. It is noted that  $\kappa$ ,  $\sigma$ , and  $L$  are all tensors, whose off-diagonal components can have non-negligible contributions in magnetic field.<sup>5,9</sup> Both  $\kappa(B)$  and  $\sigma(B)$  are measured along the same direction, which we define as  $\kappa_{xx}(B)$  and  $\sigma_{xx}(B)$ . For an anisotropic sample, even to first order, the magnetic field affects the diagonal terms of the tensors as well as the nondiagonal terms. We show that by measuring only the diagonal terms we are able to extract the Lorenz number  $L_{xx}$ ,

which relates  $\kappa_{xx}$  to  $\sigma_{xx}$ . The reason behind the validity of this method is that both  $\kappa(B)_{xx}$  and  $\sigma(B)_{xx}$  have a similar magnetic field dependence and their ratio has only a weak dependence on the off-diagonal terms. Since the samples are isotropic<sup>10</sup> and extrinsic, it is assumed that off-diagonal terms can be neglected because thermogalvanomagnetic effects are only dominant in intrinsic materials with a proportional number of positive and negative charge carriers.<sup>4,11</sup> As long as both have the same functional form with respect to the magnetic field, then  $\kappa(B)$  vs  $\sigma(B)$  will have a linear relationship, and the Lorenz number  $L_{xx}$  at a given temperature can be directly taken from the slope as given in Eq. (3). It is important to note that the analysis throughout this paper is based on the assumption that the Lorenz number is independent of magnetic field, which is true for some materials but, in general, is not a valid assumption.<sup>12–14</sup> Analogous approximations have been used to study similar compounds in the past.<sup>6,12</sup>

Neither method has been extensively used due to the fact that there are restrictions on the materials that can be measured because there must be a significant carrier contribution to the total thermal conductivity; also the experimental setup is rather difficult to realize.<sup>1,5–9</sup> The advent of the Physical Properties Measurement System (PPMS) from Quantum Design makes the experimental setup and measurement readily possible for either method. The purpose of this paper is to present experimental techniques for the determination of the Lorenz number from which both the electronic and lattice contributions to the thermal conductivity can be directly extracted. Measurements are compared to literature values as well as simple model calculations. There are several different ways to analyze the raw experimental data; two different models will be used here and are shown to yield similar results. The measurements are performed below 150 K so that bipolar terms will be negligible, and therefore Eqs. (1) and (3) accurately describe the contributions to the total thermal conductivity.

## II. EXPERIMENT

Samples were prepared by combining the proper stoichiometric ratios of Cu (99.999%, Alfa Aesar), Bi (99.999%, Alfa Aesar), Te (99.999%, Alfa Aesar), and Se (99.999%, Alfa Aesar) for  $\text{Cu}_{0.01}\text{Bi}_2\text{Te}_{2.7}\text{Se}_{0.3}$ , while  $\text{Bi}_{0.88}\text{Sb}_{0.12}$  was prepared with Bi (99.999%, Alfa Aesar) and Sb (99.999%, Alfa Aesar). Samples were then ball milled and pressed using dc hot-pressing techniques.<sup>10</sup> Metallic contacts were sputtered onto the surfaces so that electrical contacts could be soldered to the sample.

MTR measurements were performed using the thermal transport option (TTO) of the PPMS in which the sample was placed in an orientation where the magnetic field was perpendicular to the heat flow. A standard two-point method was used for thermal conductivity and Seebeck coefficient  $S$  measurements with typical sample dimensions of  $2 \times 2 \times 3 \text{ mm}^3$ . In this case the temperature was held constant at 100 K, and measurements were made while the field was swept over a range of 0.1–5 T. Since resistivity  $\rho$  values in a magnetic field are required, a four-point technique must be used, which was accomplished with the ac transport option on a different sample of dimensions  $1 \times 2 \times 12 \text{ mm}^3$  for the same temperature and field range. Since a four-point technique is used, there is no

concern of electrical contact resistance. For thermal contact resistance, our previous measurements show no difference in the thermal conductivity when a two- or four-point method is used. Even so, any thermal contact resistance is assumed to be negligible in field, and since we are looking at the change in thermal conductivity with field, there should be no influence on the slope  $L$  of the measurement. Geometrical effects on the magnetoresistance are considered to be negligible because the sample used for resistivity measurements in field has the appropriate aspect ratio. The sample dimensions for the thermal magnetoresistance measurements are restricted due to requirements to fit into the PPMS; however, it is assumed there is a negligible contribution because there was no evidence previously of geometrical effects on a similar material which had an aspect ratio of 1.<sup>12</sup> Errors for the MTR measurements of  $L$  and  $\kappa_{\text{lattice}}$  were calculated from the standard deviation and propagation of error and were determined to be 3% and 7%, respectively. Hall measurements to determine the mobility  $\mu_H$  from which the scattering factor  $r$  is obtained were made using the PPMS on the same sample as the four-point  $\rho$  measurement.

When determining the Lorenz number in a classically large field, the TTO of the PPMS in which the magnetic field was perpendicular to the heat flow was again used. A standard two-point method was used for all transport measurements on the same sample. The sample was run in magnetic fields of 0, 6, and 9 T. Only the thermal conductivity measurements in field are used, while electrical resistivity values are taken from the zero-field data. Typical sample dimensions were  $2 \times 4 \times 2 \text{ mm}^3$ . Thermal contact resistance is assumed to be negligible for the reasons stated above, and electrical contact resistance is negligible from the comparison of two- and four-point resistivity measurements. There is no concern of geometrical effects on thermal conductivity measurements because saturation would not be obtained at higher magnetic fields. The measurements were performed over a temperature range of 5–150 K, with the error for  $L$  and  $\kappa_{\text{lattice}}$  being 2% and 6%, respectively, determined from the standard deviation and propagation of error.

## III. RESULTS

The MTR approach can be used only if the thermal and electrical conductivities have the same functional form with respect to the magnetic field. Since the MTR method is used in intermediate fields, or when  $\mu B \approx 1$ , only values in magnetic fields from 0.8 to 5 T were used; anything below 0.8 T was too low of a field. The top left inset in Fig. 1 plots  $\kappa$  as a function of field, while the bottom right inset plots  $\sigma$  as a function of field for  $\text{Cu}_{0.01}\text{Bi}_2\text{Te}_{2.7}\text{Se}_{0.3}$ . Both the electrical and thermal conductivities vary with field as  $\frac{aB^2}{1+cB^2}$ , where  $a$  and  $c$  are constants, which is valid for strong degeneracy.<sup>2,16,17</sup> The fits are shown in the insets of Fig. 1 along with the measured values. Figure 1 can be fit linearly, and taking the slope yields  $LT$  in Eq. (3), from which we get  $L = 2.16 \times 10^{-8} \text{ V}^2 \text{ K}^{-2}$  by dividing by  $T = 100 \text{ K}$ . The lattice portion of the thermal conductivity is given by the  $y$  intercept and gives  $\kappa_{\text{lattice}} = 1.49 \text{ W mK}^{-1}$ . Care should be taken with the determination of  $\kappa_{\text{lattice}}$  this way because a larger error is induced when extrapolating over six orders of magnitude to

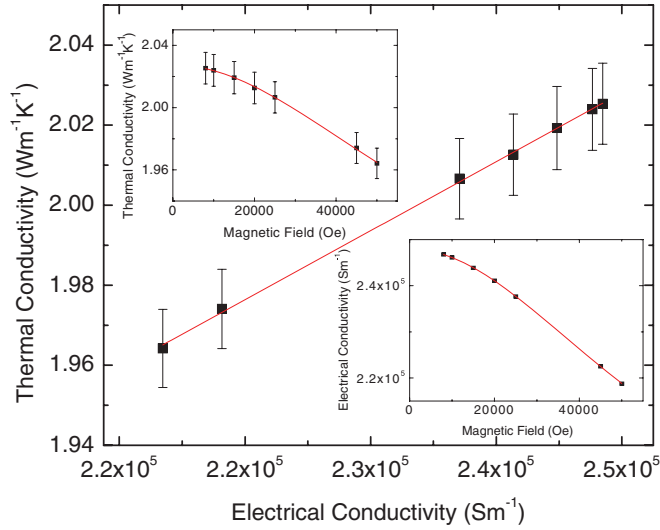


FIG. 1. (Color online) Thermal conductivity is plotted against electrical conductivity of  $\text{Cu}_{0.01}\text{Bi}_2\text{Te}_{2.7}\text{Se}_{0.3}$  at 100 K with the magnetic field being varied from 0.8 to 5 T. The slope of the linear fit provides the Lorenz number  $L = 2.16 \times 10^{-8} \text{ V}^2 \text{ K}^{-2}$ , and the y intercept gives  $\kappa_{\text{lattice}} = 1.49 \text{ W mK}^{-1}$ . The top left inset plots the dependence of the total thermal conductivity on magnetic field. The bottom right inset plots the dependence of electrical conductivity on magnetic field. Both the thermal conductivity and electrical conductivity varying with field can be fit using  $\frac{aB^2}{1+cB^2}$ , as shown in the insets.

get  $\kappa_{\text{lattice}}$  when  $\sigma(B)$  is zero. If  $\kappa_{\text{carrier}}$  is calculated from the Lorenz number and the electrical conductivity in zero field,  $\kappa_{\text{lattice}}$  can be calculated from  $\kappa_{\text{total}} - \kappa_{\text{carrier}}$ , which gives a value of  $1.35 \text{ W mK}^{-1}$ . For a comparison with the measured values, a simple model for the calculation of the Lorenz number is given by<sup>3</sup>

$$L = \left(\frac{k_B}{e}\right)^2 \left[ \frac{(r + 7/2)F_{r+5/2}(\xi)}{(r + 3/2)F_{r+1/2}(\xi)} - \left( \frac{(r + 5/2)F_{r+3/2}(\xi)}{(r + 3/2)F_{r+1/2}(\xi)} \right)^2 \right], \quad (4)$$

where  $r$  is the scattering parameter,  $k_B$  is Boltzmann's constant,  $e$  is the electron charge, and  $F_n(\xi)$  is the Fermi integral given by

$$F_n(\xi) = \int_0^\infty \frac{\chi^n}{1 + e^{\chi - \xi}} d\chi, \quad (5)$$

where  $\xi$  is the reduced Fermi energy that can be calculated from the Seebeck coefficient  $S$  as well as the scattering parameter  $r$ , which is given by

$$S = \pm \frac{k_B}{e} \frac{(r + 5/2)F_{r+3/2}(\xi)}{(r + 3/2)F_{r+1/2}(\xi)} - \xi. \quad (6)$$

In this model the Lorenz number can be calculated with knowledge of the Seebeck coefficient and the scattering parameter, both of which were measured at 100 K. The insets of Fig. 2 show  $\mu_H$  plotted as a function of temperature over the entire temperature range (top left) as well as only the data around 100 K (bottom right), which were used to calculate the scattering parameter  $r$ . The data in Fig. 2 are for

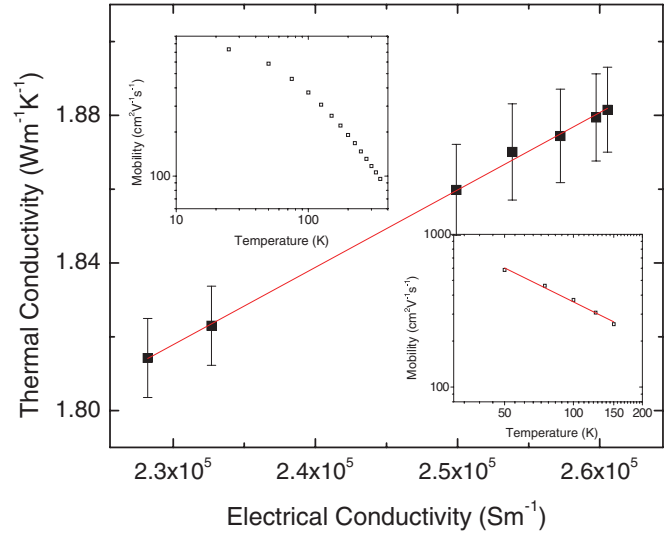


FIG. 2. (Color online) Thermal conductivity is plotted against electrical conductivity of  $[\text{Cu}_{0.01}\text{Bi}_2\text{Te}_{2.7}\text{Se}_{0.3}]_{0.98}\text{Ni}_{0.02}$  at 100 K with the magnetic field being varied from 0.8 to 5 T. The slope of the linear fit provides the Lorenz number  $L = 2.33 \times 10^{-8} \text{ V}^2 \text{ K}^{-2}$ , and the y intercept gives  $\kappa_{\text{lattice}} = 1.27 \text{ W mK}^{-1}$ . The top left inset plots  $\ln(\mu_H)$  vs  $\ln(T)$  over the whole temperature range. The bottom right inset plots only the points in the vicinity of 100 K from which the slope is taken to derive the scattering parameter.

$[\text{Cu}_{0.01}\text{Bi}_2\text{Te}_{2.7}\text{Se}_{0.3}]_{0.98}\text{Ni}_{0.02}$ ; the same method was used to calculate  $r$  for  $\text{Cu}_{0.01}\text{Bi}_2\text{Te}_{2.7}\text{Se}_{0.3}$ . The scattering parameter  $r$  was determined by taking the slope of  $\ln(\mu_H)$  vs  $\ln(T)$  around 100 K, using the relationship  $\mu \propto T^{r-1}$ .<sup>15</sup> The values for the mobility were nearly identical between the two samples, with values for  $r$  being 0.26 and 0.27 for  $\text{Cu}_{0.01}\text{Bi}_2\text{Te}_{2.7}\text{Se}_{0.3}$  and  $[\text{Cu}_{0.01}\text{Bi}_2\text{Te}_{2.7}\text{Se}_{0.3}]_{0.98}\text{Ni}_{0.02}$ , respectively. Though there is some error induced in the determination of  $r$  because the scattering parameter in general changes with temperature, these values should be more accurate than the commonly assumed  $r = -1/2$  for acoustic phonon scattering. This fact is seen in the calculated values for  $L$  where using  $r = -1/2$  yields values of  $L$  that are 3% higher than when  $r$  is calculated from the mobility. The calculated value using Eqs. (4)–(6) and  $r = 0.26$  gives  $L = 2.34 \times 10^{-8} \text{ V}^2 \text{ K}^{-2}$  and  $\kappa_{\text{lattice}} = 1.30 \text{ W mK}^{-1}$ , both of which are close to the experimentally determined values.

The same procedure was followed for  $[\text{Cu}_{0.01}\text{Bi}_2\text{Te}_{2.7}\text{Se}_{0.3}]_{0.98}\text{Ni}_{0.02}$ , and Fig. 2 shows again that  $\kappa(B)$  vs  $\sigma(B)$  is linear. The measured value for the slope gives  $L = 2.33 \times 10^{-8} \text{ V}^2 \text{ K}^{-2}$ , and from the y intercept  $\kappa_{\text{lattice}} = 1.27 \text{ W mK}^{-1}$ . The calculated values using Eqs. (4)–(6) give  $L = 2.36 \times 10^{-8} \text{ V}^2 \text{ K}^{-2}$  and  $\kappa_{\text{lattice}} = 1.13 \text{ W mK}^{-1}$ , again showing the validity of the measurement. Besides the MTR method the data can also be fit using the following expressions for the electrical and thermal conductivities as a function of field for isotropic samples in the relaxation-time approximation:<sup>18</sup>

$$\sigma(B) = \frac{\sigma_0}{1 + (\mu_d B)^2}, \quad (7)$$

$$\kappa(B) = \kappa_{\text{lattice}} + \frac{\kappa_{\text{carrier}}}{1 + (\mu_d B)^2}, \quad (8)$$

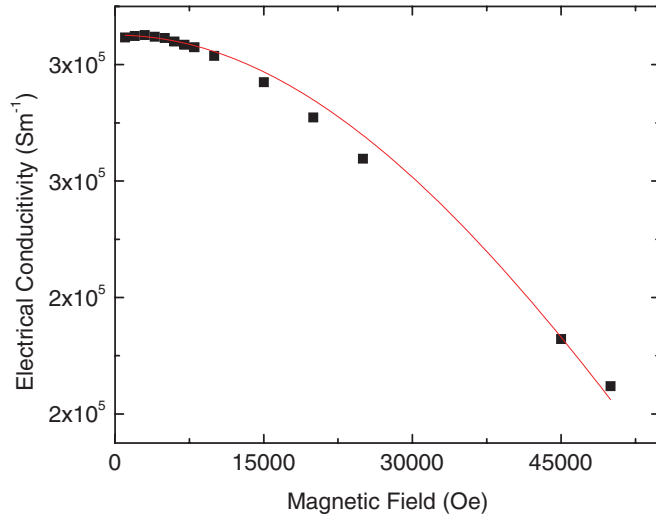


FIG. 3. (Color online) Electrical conductivity is plotted against magnetic field from 0.1 to 5 T and fit using Eq. (7). The electrical conductivity in zero field is used in order to determine the drift mobility  $\mu_d$ .

where  $\sigma_0$  is the electrical conductivity in zero field and  $\mu_d$  is the drift mobility. The drift mobility determined by Eq. (7) and shown in Fig. 3 is used in Eq. (8) in order to determine the carrier and lattice contributions to the thermal conductivity, as shown in Fig. 4. As opposed to the MTR method, the data must be fit using both weak and intermediate magnetic fields, and so Figs. 3 and 4 show the thermal and electrical conductivities in fields of 0.1–5 T. Fitting Eq. (8) to the thermal conductivity vs magnetic field data in Fig. 4 yields  $\kappa_{\text{lattice}} = 1.29 \text{ W mK}^{-1}$ . It can be seen that using the completely different model presented in Eqs. (7) and (8) produces a nearly identical value of  $\kappa_{\text{lattice}} = 1.27 \text{ W mK}^{-1}$  as determined by the MTR method.

Unlike  $\text{Cu}_{0.01}\text{Bi}_2\text{Te}_{2.7}\text{Se}_{0.3}$ , it was possible to reach the classical high-field limit at lower temperatures for bismuth antimony compounds. Figure 5 plots the thermal conductivity

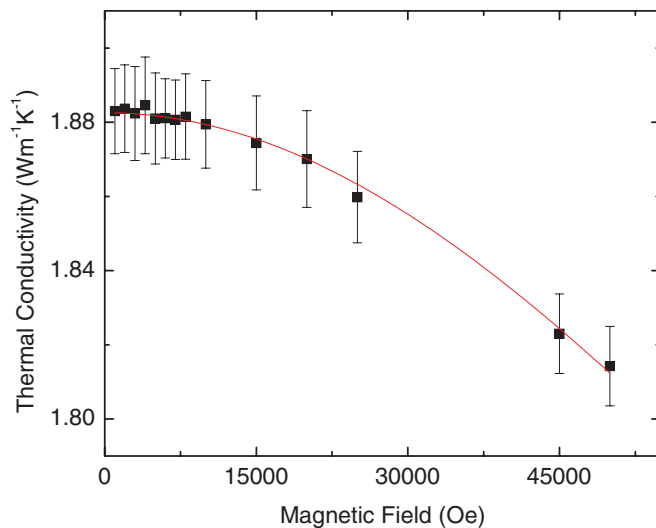


FIG. 4. (Color online) Thermal conductivity is plotted against magnetic field from 0.1 to 5 T and fit using Eq. (8) and  $\mu_d$  from Fig. 3. It is found that  $\kappa_{\text{lattice}} = 1.29 \text{ W mK}^{-1}$ .

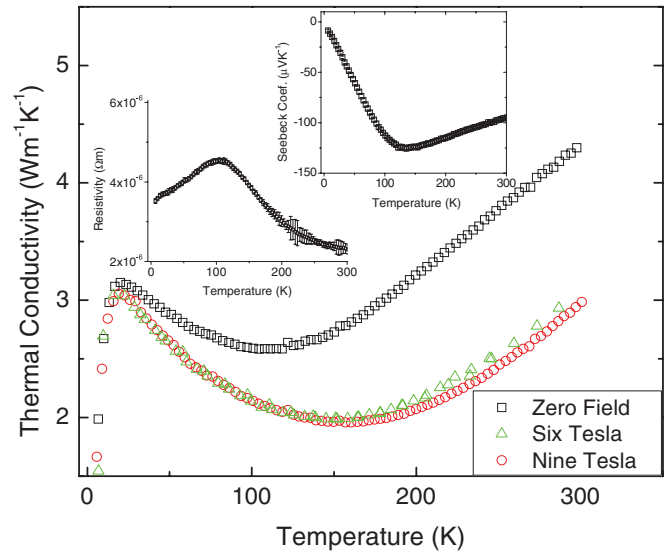


FIG. 5. (Color online) Thermal conductivity is plotted against temperature at magnetic fields of 0, 6, and 9 T for  $\text{Bi}_{0.88}\text{Sb}_{0.12}$ . The top right inset plots the Seebeck coefficient against temperature, while the top left inset plots  $r$  vs  $T$  from 5 to 300 K in zero magnetic field. It can be clearly seen that the bipolar contribution to the Seebeck coefficient becomes non-negligible around 150 K.

of  $\text{Bi}_{0.88}\text{Sb}_{0.12}$  vs temperature in magnetic fields of 0, 6, and 9 T. The fact that the field is classically large in the temperature range of 5–150 K can be seen by inspection of Fig. 5. Since there is no change when increasing the field from 6 to 9 T below 150 K, the high-field limit has been reached, and  $\kappa_{\text{carrier}}$  has been completely suppressed. As can be seen in Fig. 5, the onset of the bipolar effect occurs above 150 K but not radiation effects since these are negligible under 200 K, which is not eliminated by the magnetic field and results in both the increase of the thermal conductivity and the lack of suppression of  $\kappa_{\text{carrier}}$ . The zero-field values for the Seebeck coefficient and electrical resistivity are plotted in the insets, both of which confirm the onset of bipolar effects around 150 K. The fact that the electronic thermal conductivity is not suppressed due to the bipolar contribution has been described by Uher and Goldsmid, and in pure bismuth happens at around 150 K.<sup>5</sup> Therefore, extraction of the Lorenz number using this method is only possible for temperatures below 150 K, where bipolar contributions are negligible. Once the lattice and total thermal conductivities are measured, the electronic portion was calculated using Eq. (1). Equation (2) can be rewritten as  $LT = \kappa_{\text{carrier}}\rho$ , where  $\rho$  is the zero-field value for the electrical resistivity. Since, in this case, the lattice portion is measured over a range of temperatures,  $\kappa_{\text{carrier}}\rho$  can be plotted versus temperature, and the slope of the line will yield  $L$  for that temperature range. Figure 6 shows only the portion of the temperature range over which the plot is linear. At higher temperatures, above 150 K, the classical field approximation is no longer valid due to a drastic decrease in mobility as well as the onset of the bipolar contribution,<sup>5,7</sup> while at lower temperatures  $\kappa_{\text{lattice}}$  dominates and therefore  $\kappa_{\text{total}}$  is unaffected by magnetic field, as can be seen in Fig. 5. Fitting linearly, as shown in Fig. 6, gives the measured value for the Lorenz number as  $2.21 \times 10^{-8} \text{ V}^2 \text{ K}^{-2}$  in the

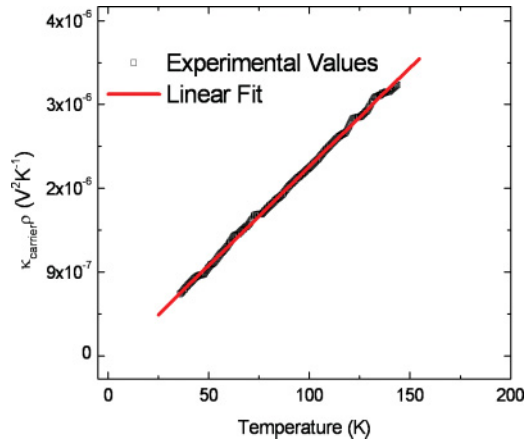


FIG. 6. (Color online)  $\kappa_{\text{carrier}}\rho$  is plotted against temperature from 35 to 150 K. The black points represent the measured data, while the red line is the linear fit. The slope of the linear fit provides the Lorenz number  $L = 2.21 \times 10^{-8} \text{ V}^2 \text{ K}^{-2}$ , and the y intercept gives  $\kappa_{\text{lattice}} = 2.14 \text{ W mK}^{-1}$ .

temperature range 35–150 K, meaning  $L$  is constant over this range of temperature. Sharp *et al.* measured a sample of identical composition in fields up to 1 T, where they were unable to reach the high-field limit and therefore used the MTR method described above.<sup>6</sup> They obtained  $L = 2.31 \times 10^{-8} \text{ V}^2 \text{ K}^{-2}$  at 100 K, which is less than a 5% difference from our measurement. When comparing values for the lattice portion of the thermal conductivity, our measured value at 100 K yields  $2.14 \text{ W mK}^{-1}$ , while the value determined using the MTR method from extrapolation is  $2.19 \text{ W mK}^{-1}$ .<sup>6</sup> It should be noted that the grain sizes in both samples are of the same order of magnitude, with average grain sizes being roughly 1 and  $5 \mu\text{m}$  for our sample and that of Sharp, respectively.<sup>6</sup> Again, as in the low-field limit, the measured values are not only reasonable but also within 5% of published values on the same material.

#### IV. DISCUSSION

There is excellent agreement between the two models used to fit the data in the low-field limit for  $\text{Cu}_{0.01}\text{Bi}_2\text{Te}_{2.7}\text{Se}_{0.3}$  and  $[\text{Cu}_{0.01}\text{Bi}_2\text{Te}_{2.7}\text{Se}_{0.3}]_{0.98}\text{Ni}_{0.02}$  as well as decent agreement with simple parabolic band model theory. There is also excellent agreement between both low- and high-field methods, as shown in the measurements of  $\text{Bi}_{0.88}\text{Sb}_{0.12}$  and their comparison with literature values. While measurements for  $\text{Bi}_{0.88}\text{Sb}_{0.12}$  were made near the typical temperature range of operation, these temperatures are far from optimal for  $\text{Cu}_{0.01}\text{Bi}_2\text{Te}_{2.7}\text{Se}_{0.3}$ , which operates in a much higher temperature range.<sup>10</sup> The purpose of measuring  $\text{Cu}_{0.01}\text{Bi}_2\text{Te}_{2.7}\text{Se}_{0.3}$  was to see first if the measurement was possible in nanostructured materials and second to see how high the temperature could be raised while performing the measurement. Therefore the measurement was also tried at 250 K; however, there was no variation in the thermal conductivity data outside of experimental error. This is due to the fact that the mobility decreased by a factor of 3 at 250 K.

The requirement of high mobility is one of the limitations of this technique. Other limitations include the requirements

for a high magnetic field, again to satisfy  $\mu B \gg 1$ , as well as the electronic portion of the thermal conductivity being at least 5%. Ideal thermoelectric materials will have a high mobility along with a low lattice thermal conductivity, which is comparable to the electronic portion, and so the use of magnetic field to separate out  $\kappa_{\text{carrier}}$  would be perfect for the ideal nanostructured thermoelectric material.<sup>1,5–9</sup> The assumptions that are being made for the analysis (models used to fit the data) using this method are that the Lorenz number is independent of magnetic field, the lattice is unaffected by magnetic field, there is no bipolar contribution, and electron-phonon interactions are negligible. The assumption that the Lorenz number and lattice are independent of magnetic field is true for some materials, which we take to be the case for these materials,<sup>12</sup> but in general it is not true and can be affected by secondary magnetic impurities. We are investigating the generality of this assumption further. Bipolar contributions should be negligible at 100 K. We assume electron-phonon interactions would manifest themselves when comparing the high- and low-field methods in  $\text{Bi}_{0.88}\text{Sb}_{0.12}$ . In the high-field limit the carrier completes a full orbit and therefore should be more likely to scatter a phonon, which would lead to a difference in the thermal conductivity between the high- and low-field measurements. Since there is no difference between the two methods, we believe the electron-phonon interactions to be negligible. It is noted that it would be interesting to devise an experiment from which electron-phonon interactions could be determined.

Because of the limitations on the material, only metals (W,<sup>13</sup> Cu,<sup>19</sup> Pb,<sup>20</sup> Rb,<sup>21</sup> etc.) along with a few alloyed compounds [ $\text{Cd}_3\text{P}_2$  (Ref. 22) and  $\text{Cd}_3\text{As}_2$  (Ref. 23)] have been measured using magnetic field; what we have found is referenced here and throughout the paper. Review articles written by Butler and Williams<sup>17</sup> and, more recently, by Kumar<sup>1</sup> attempt to give several literature values, though many were missed, for the Lorenz number of different elements and alloys determined by all types of experimental methods, not just in magnetic field. Another example of experimentally determining the Lorenz number is through the introduction of impurities in alloys, where the change in electrical conductivity and  $\kappa_{\text{carrier}}$  is used to determine  $\kappa_{\text{lattice}}$ . A nice description, with examples as well as shortcomings, of the alloying method is given by Butler and Williams.<sup>17</sup>

Further investigation is required into higher-temperature measurements as well as other types of materials<sup>14,24</sup> for which this technique can be useful. It should also be mentioned that we have only looked at the diagonal components, specifically  $\kappa_{xx}$  and  $\sigma_{xx}$ , of the transport tensors, and it could be possible to extract even more data from the off-diagonal components through measurements of the Righi-Leduc and Hall coefficients.<sup>24,25</sup> Future work will include systematic measurements of the transport tensors on a specific material over a larger temperature range along with more complex theoretical analysis.

#### V. CONCLUSION

Two methods for experimentally determining the Lorenz number are presented for nanopolycrystalline  $\text{Bi}_{0.88}\text{Sb}_{0.12}$ ,  $\text{Cu}_{0.01}\text{Bi}_2\text{Te}_{2.7}\text{Se}_{0.3}$ , and  $[\text{Cu}_{0.01}\text{Bi}_2\text{Te}_{2.7}\text{Se}_{0.3}]_{0.98}\text{Ni}_{0.02}$ .

Measured values of  $\text{Cu}_{0.01}\text{Bi}_2\text{Te}_{2.7}\text{Se}_{0.3}$  and  $[\text{Cu}_{0.01}\text{Bi}_2\text{Te}_{2.7}\text{Se}_{0.3}]_{0.98}\text{Ni}_{0.02}$  analyzed using Eqs. (1)–(3) as well as Eqs. (7) and (8) yield similar results and are close to calculated values using the single parabolic band model presented in Eqs. (4)–(6). The measured values for  $\text{Bi}_{0.88}\text{Sb}_{0.12}$  are the same as previously published results. Now that the two methods have been clearly demonstrated to work on these nanopolycrystalline alloys at a given temperature, it is possible to look at other materials as well as the temperature range for which this technique can be used. A systematic study can then be done of the temperature dependence of the Lorenz number for a given material, making it possible

for more complex theoretical models to be verified within experimental error, leading to more accurate determinations of the lattice portion of the thermal conductivity.

#### ACKNOWLEDGMENTS

This work is supported by the “Solid State Solar-Thermal Energy Conversion Center (S3TEC),” an Energy Frontier Research Center founded by the US Department of Energy, Office of Science, Office of Basic Energy Science, under Award No. DE-SC0001299/DE-FG02-09ER46577.

<sup>1</sup>G. S. Kumar and M. E. Fine, *J. Mater. Sci.* **28**, 4261 (1993).

<sup>2</sup>S. A. Aliev, L. L. Korenblit, and S. S. Shalyt, *Sov. Phys. Solid State* **8**, 565 (1966).

<sup>3</sup>D. M. Rowe and C. M. Bhandari, *Modern Thermoelectrics* (Reston Publishing, Reston, VA, 1983).

<sup>4</sup>N. Hsieh and M. E. Fine, *J. Appl. Phys.* **52**, 2876 (1981).

<sup>5</sup>C. Uher and H. J. Goldsmid, *Phys. Status Solidi B* **65**, 765 (1974).

<sup>6</sup>J. W. Sharp, E. H. Volckmann, and H. J. Goldsmid, *Phys. Status Solidi A* **185**, 257 (2001).

<sup>7</sup>D. Armitage and H. J. Goldsmid, *J. Phys. C* **2**, 2138 (1969).

<sup>8</sup>G. K. White and S. B. Woods, *Philos. Mag.* **3**, 342 (1958).

<sup>9</sup>R. T. Delves, *Br. J. Appl. Phys.* **15**, 105 (1964).

<sup>10</sup>W. S. Liu, Q. Zhang, Y. Lan, S. Chen, X. Yan, Q. Zhang, H. Wang, D. Z. Wang, G. Chen, and Z. F. Ren, *Adv. Energy Mater.* **1**, 577 (2011).

<sup>11</sup>D. M. Rowe, *CRC Handbook of Thermoelectrics* (CRC Press, New York, 1995).

<sup>12</sup>A. E. Bowley, R. Delves, and H. J. Goldsmid, *Proc. Phys. Soc. London* **72**, 401 (1958).

<sup>13</sup>J. De Nobel, *Physica* **15**, 532 (1949).

<sup>14</sup>M. R. Stinson, R. Fletcher, and C. R. Leavens, *Phys. Rev. B* **20**, 3970 (1979).

<sup>15</sup>A. F. Ioffe, *Physics of Semiconductors* (Infosearch, London, 1960).

<sup>16</sup>R. Laiho, S. A. Némov, A. V. Lashkul, E. Lakhderanta, T. E. Svechnikova, and D. S. Dvornik, *Semiconductors* **41**, 546 (2007).

<sup>17</sup>W. H. Butler and R. K. Williams, *Phys. Rev. B* **18**, 6483 (1978).

<sup>18</sup>C. Jacoboni, *Theory of Electron Transport in Semiconductors* (Springer, Berlin, 2010).

<sup>19</sup>R. W. Arenz, C. F. Clark, and W. N. Lawless, *Phys. Rev. B* **26**, 2727 (1982).

<sup>20</sup>L. J. Challis, J. D. N. Cheeke, and P. Wyder, *Phys. Rev.* **143**, 499 (1966).

<sup>21</sup>R. Fletcher and I. B. Verma, *Phys. Rev. B* **36**, 9482 (1987).

<sup>22</sup>F. A. P. Blom and J. W. Burg, *J. Phys. Chem. Solids* **38**, 19 (1977).

<sup>23</sup>F. A. P. Blom and A. Huyser, *Sol. State Commun.* **7**, 1299 (1969).

<sup>24</sup>M. Matusiak, T. Plackowski, and W. Sadowski, *Sol. State Commun.* **132**, 25 (2004).

<sup>25</sup>Y. Zhang, N. P. Ong, Z. A. Xu, K. Krishana, R. Gagnon, and L. Taillefer, *Phys. Rev. Lett.* **84**, 2219 (2000).